JOURNAL OF AIRCRAFT
Vol. 44, No. 2, March–April 2007

Geometric Properties of Parachutes Using 3-D Laser Scanning

Calvin K. Lee*
U.S. Army Soldier Systems Center, Natick, Massachusetts 01760
and
Peng Li†
Geo-Centers, Inc., Natick, Massachusetts 01760

DOI: 10.2514/1.18387

The technology of gliding parafoils is currently being pursued by the U.S. Army for precision airdrop of cargos and personnel. The performance of parafoils (lift and drag) and round parachutes (drag) is closely related to their 3-D geometry. There have been some studies on the geometry of round parachutes, but hardly any on parafoils. The technology of 3-D whole body scanning provides a viable tool to investigate the 3-D geometry of parachutes. In this paper, we present an investigation on the 3-D geometry, surface area and volume of small-scale models of parafoil, round parachute, ring-slot parachute, and cross parachute using a 3-D laser scanning apparatus. Scan data from these model parachutes were obtained in a climatic chamber with a steady air velocity. Surface areas and volumes of these parachutes were calculated from the scan data using specially developed mathematical methods. In addition, cross sections of the parachute canopies were obtained from the scan images. These cross sections provide valuable information on the relationship between model parachutes and full-scale parachutes, fabric properties on canopy geometry, and parachute canopy design and manufacturing.

Introduction

PARACHUTES have been used extensively for airdrop of personnel and cargos by the United States military as well as by civilians in recreational and sport jumping. The two most common types of parachutes used are round parachutes and rectangular-shaped parafoils. The former captures air and provides a drag force to decelerate a payload to a steady descent velocity. The latter, by virtue of its design with air inflated airfoil shaped cells, provides a lift force as well as a drag force. Hence, parafoils can be steered to deliver payloads accurately on the ground. Based on this capability, parafoils are currently actively pursued by the military for precision aerial delivery of cargos [1]. Because both of the drag and lift forces of an object depend on its geometric shape, the 3-D shape of a parachute is an important parameter for the performance of a parachute. In addition, the air volume/mass enclosed by the parachute canopy (included mass) becomes part of the total parachute mass when the parachute is fully inflated [2]. As such, the included mass is also an important parameter for round parachutes and parafoils. The included air mass is part of an overall added air mass that also includes the air mass entrained outside the parachute canopy. It is the total overall added air mass that affects the motion of a parachute. The present investigation concentrates only on the included air mass; the entrained air mass is beyond the scope of this investigation. For general description and background of parachutes, readers are referred to Cockrell [2] and Knacke [3].

Because of the time consuming and expensive full-scale testing of parachutes, analytical prediction of parachute geometry and performance using coupled computational fluid dynamics (CFD) and structural dynamics [fluid/structure interaction (FSI)] computer modeling techniques have made significant advances recently [4–6]. However, FSI computer models have to be verified and validated first before they can be used reliably. For verification and validation of the models [7], measurements and experimental data are needed. Experimental investigation on the 3-D geometry of parachutes has been scarce, particularly on parafoils. Both Heinrich [8] and Berndt [9] used high-speed movies to study the geometry of model and full-scale round parachutes. Matos et al. [10] investigated the lift and drag forces of a model parafoil as a function of geometry using a photogrammetry technique with four video cameras. The well-developed technology of 3-D whole body scanning digitizers [11] presents a viable capability to investigate the steady-state 3-D geometry of fully inflated parachutes. In this paper, we present an investigation of the 3-D geometry of model parachutes using a laser scanning apparatus. Geometric representation, surface areas and volumes of small-scale models of parafoil, round parachute, ring-slot parachute, and cross parachute are presented. In addition, cross sections of the parachute canopies were obtained, many of them for the first time. They present useful results and implications on the effects of fabric properties on parachute performance, and on using model parachutes for full-scale parachute performance prediction.

Received 27 June 2005; revision received 4 January 2006; accepted for publication 23 February 2006.

*Research Aerospace Engineer, Airdrop/Aerial Delivery Directorate.
†Senior Scientist.

Experiments

3-D Laser Scanning Apparatus

The 3-D laser scanning apparatus at the U.S. Army Natick Soldier Center (NSC) has been used extensively for the anthropometric study of humans for Army clothing and helmet design [12], and most recently for the air gap investigation of flame/thermal protective clothing systems [13]. The scanning apparatus consists of four scan heads positioned on a horizontal plane diagonally from each other (Fig. 1). Each head emits a stripe of laser light onto one quadrant of the object being scanned. Two offset lenses in each head triangulate the laser light on the object. Triangulation of the deformed light on the object surface determines the surface geometry of the object. The four heads travel vertically downward and simultaneously as they scan the object. By integrating the scan data from the four scan heads, a complete 360-degree 3-D geometry of the object is determined. The scanning apparatus covers a maximum vertical cylindrical volume of 1.2-m diam and 2-m height. For this scanning volume, the maximum size for a round parachute is about 1.3 m in diameter, and for a parafoil about 1.6-m in wing span (in the vertical direction). Figure 1 shows an inflated 1.5-m wing-span parafoil being scanned by the four scan heads.

For each camera in the scan head, the scan resolution is 5 mm horizontally (X direction in the right-handed XYZ coordinates), 0.5 mm in depth (Y direction) and 2 mm vertically (Z direction). The simultaneous scans by the four cameras do not decrease the vertical and in-depth resolution, but does decrease the horizontal resolution

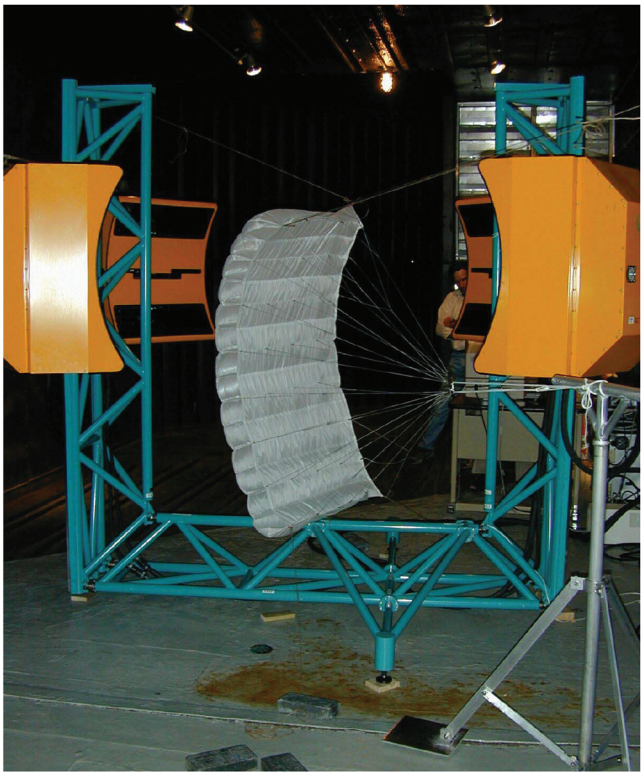

Fig. 1 Inflated model parafoil being scanned by the laser scanning system.

to 3 mm. One can see that errors resulting from the inherent limitations of the cameras are very small in the three dimensions of the maximum vertical cylindrical volume. However, when a three-dimensional object is being scanned, the surface contour of the object dictates the ability of the laser beam to reach the object surface to obtain a high-quality scan. For example, a curved surface or a sharp corner, such as those of a parachute canopy, will limit the laser beam to obtain a maximum number of scans for accurate surface area and volume determination. As a result, special mathematical methods and computer software will be needed to determine the geometry. Therefore, object-dependent errors will have to be determined individually for each object. This type of error will be discussed in the remainder of this section and the next one.

Model Parachutes

For this investigation, small-scale models of a parafoil, three solid-cloth round parachutes, a ring-slot parachute, and three cross parachutes were constructed. Their dimensions and construction details are shown in Table 1. It has been shown that for large-scale parachute performance simulation, more flexible and permeable and lighter canopy fabrics than those of full-scale parachute canopies are needed for small-scale model parachutes [14]. However, such fabrics are currently unavailable commercially. Therefore, the nylon used for full-scale parachutes was used for the models. However, much lighter reinforcing tapes and suspension lines were used based on the guidelines presented in previous work [15]. Naturally, geometric similarity between full-scale and model parachutes was preserved. As indicated in Table 1, the parafoil is a 1/3-scale model of a 4.5-m wing-span personnel parafoil. The other parachutes are not models of any particular full-scale parachutes, but are typical model parachutes for laboratory studies.

Parachute Scanning

The 3-D laser scanning apparatus was set up in the test section of the Tropic Doriot Climatic Chamber at the NSC. Dimensions of the test section are 4.6 m high, 3.3 m wide, and 6.7 m long, which adequately accommodated the scanning apparatus. All scans were conducted at a room temperature of 70°C and air velocity of 6.7 m/s. Using 1 m as a representative characteristic length for the parachutes (see Table 1), the Reynolds number for the test condition was on the order of 447,000. At higher velocities, oscillation of the inflated parachute canopies and the flutter of the canopy fabric were too excessive for the apparatus to obtain an accurate scan of the canopies. As shown in Fig. 1, the parafoil was held in place by a metal frame and inflated vertically. To minimize the movement of the parafoil during scanning, thin threads were attached to its four corners and tied to the chamber wall. These experimental procedures worked well and improved the surface scanning process. However, due to the sharp edges of the parafoil and the scalloped shape of the cells, the laser beams were not able to reach some of the surface areas, such as the end cells and some joined areas between adjacent cells. This resulted in some blind spots or void areas in the scan. These experimental procedures used for the parafoil were also used and worked well for the round, ring slot and cross parachutes. Similar to the parafoil, void areas were also encountered in their scans. Figure 2 shows these parachutes being scanned by the four scan heads.

To account for these void areas in the geometric determination of the parachutes, mathematical methods and computer software had to be developed. Because of the different geometry of the parafoil from that of the other round parachutes, two different mathematical schemes were developed for the two types of parachutes. The scheme for the parafoil was less involved than that for the round parachutes and is described later. The more involved scheme for the round parachutes has been reported elsewhere [16] and it will be only briefly described in this paper.

Surface Area and Volume Calculations

Surface Representation

Data collected from the 3-D scanner are a cloud of points. A surface modeling methodology is required for calculating surface area and volume from these points. A method based on triangular

Table 1 Dimensions and construction of model parachutes

Parafoil (1/3-scale model of a personnel parafoil	Wing span m 1.5	Length m 0.76	No. of cells 14	Canopy fabric aerial density g/m^2 33.9
Round parachute (RP)	Constructed diameter m	No. of gores	Canopy fabric aerial density g/m^2	
RP1	1.17	24	33.9	
RP2	1.22	14	33.9	
RP3	1.22	14	33.9 (nonporous)	
Ring slot parachute	1.22	14 (3 rings)	33.9	
Cross parachute (CP)	Arm length/width m/m	Vent	Web	Canopy fabric areal density g/m^2
CP1	0.582/0.198	Yes	No	77
CP2	0.582/0.198	No	No	77
CP3	0.582/0.198	No	Yes	77

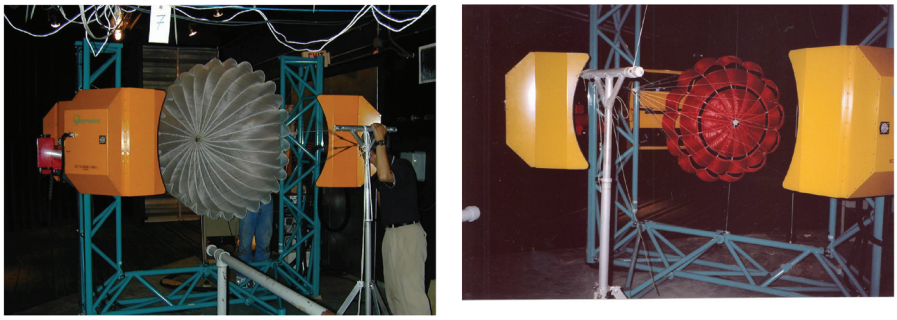

a) b)

Fig. 2 Inflated round parachute a) and ring-slot parachute b) being scanned by the laser scanning system.

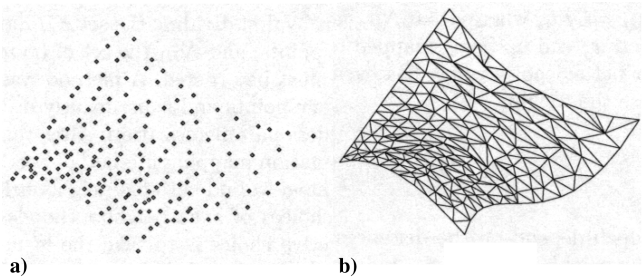

a) b)

Fig. 3 Typical cloud of points scanned from the surface of an object a); corresponding triangular mesh geometry b).

mesh geometry was developed for the parafoil and a method based on contour geometry was developed for the round parachutes.

Mesh-Based Surface

The mesh geometry represents a surface as a field indexed by mesh elements. A triangular mesh connects three spatial points into a planer triangle as illustrated in Fig. 3. There are established surface reconstruction algorithms aiming to construct a meaningful surface from a 3-D point cloud [17–19]. Our surface reconstruction method relies on the image coordinates obtained from the image sensors of the four scanners. Neighborhood information of the 3-D spatial points can be determined from the image coordinates, which eliminates ambiguity during 3-D triangulation. Although the image coordinates help to define a spatial relationship, a reconstructed surface contains voids due to lack of data. These voids are manually filled to make a surface complete.

The volume of a meshed surface has been investigated by the digital terrain modeling technique. In this technique, a triangulated irregular network (TIN) is used to represent the terrain surface and the total volume enclosed between the TIN and a zero elevation planer (floor) is estimated by summing the volume of each triangular prism. Figure 4 illustrates a TIN and its volume. A parafoil cell is similar to a TIN but with two surfaces and without a planer floor. To apply the TIN volume approach to the parafoil cells, a simple solution is to supply a virtual floor to a parafoil cell. The floor has to

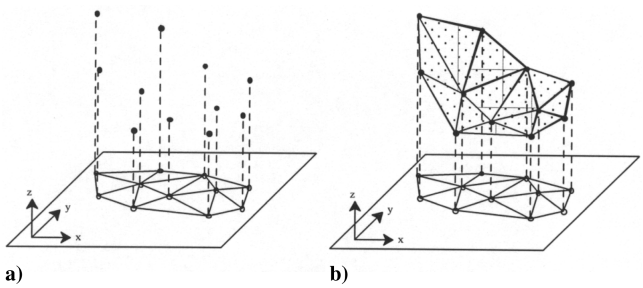

a) b)

Fig. 4 a) Terrain surface represented by a triangulated network; b) triangular prisms formed between the terrain surface and a planer floor.

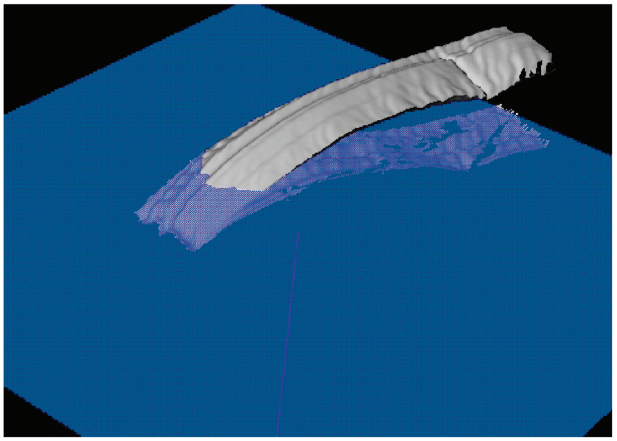

Fig. 5 Parafoil cell surface and its virtual planer floor.

be as parallel as possible to the tangent planes of the upper and lower surfaces of the cell.

To find the best fitting plane to the upper and lower surfaces of the cell, its principal axes are computed and the floor plane is chosen as the plane with a maximum projected surface area. However, the floor plane is most likely located between the upper and lower surfaces and may have both sections on the one side at the rear of the cell as shown in Fig. 5. When the upper and lower surfaces are on the opposite side of the floor, the volumes will be added. When the upper and lower surfaces are on the same side of the floor, one of their volumes will be subtracted from the other.

Contour-Based Surface

The contour-based surface model has been widely used for 3-D reconstruction from boundary data [20]. It models a surface as a set of parallel cross-sectional curves and the approach is most suitable for cylindrical shaped objects (Fig. 6). The contour-based modeling method was used for the 3-D scans of the round parachutes for 1) filling void areas at each cross-sectional level, and 2) for eliminating data noise due to parachute vibration during scanning. After the contour fitting, the surface area and volume of an inflated parachute are determined by numerical integration. The surface area is obtained from the integration of the arc length of contours and volume from the integration of the enclosed planer area of contours. The numerical integration approach, together with a B-spline curve fitting function, acts as a strong low pass filter and produces robust, consistent results. Details of this method have been published [16].

Apparatus Calibration

To check the accuracy of the 3-D scanning apparatus and the two surface modeling methods, a solid circular cylinder with dimensions of 24.9 cm in diameter and 25 cm in height was scanned with the height in the vertical position. Its surface area and volume were

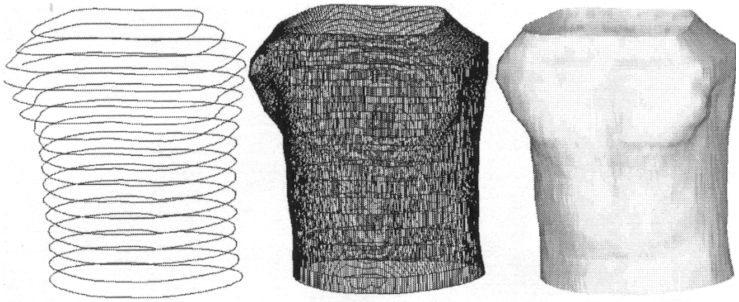

Fig. 6 Contour representation of a surface.

calculated using the mesh-based and the contour-based methods. Results are shown in Table 2.

Compared with the theoretical values, both methods give an error of less than 1% for the surface area and less than 1.5% for the volume. In the actual scanning of parachutes, surface voids and vibration as described earlier introduce additional uncertainties. Unlike the well-defined solid circular cylinder, theoretical values of the parachute canopies have their own uncertainties already due to the flexibility and stretching of the fabric. The best one could do is to fill the surface voids with optimum representation and average the scan measurements.

Results

Parafoil

Three typical images of the parafoil from the scan are shown in Fig. 7. The void areas described earlier are shown as dark spots in the images. From these 3-D images, cross sections of the inflated parafoil were obtained and are shown in Fig. 8. In addition, the outline of the parafoil's rib used to separate each cell from the parafoil design drawings is also shown for comparison. It is seen that the cross sections of the inflated cells follow the shape of the airfoil design very well. As expected, the trailing edge curves downward due to the lower pressure difference there across the top and bottom surfaces, typical for a parafoil. Other than this minimal difference, the closeness between the inflated shape and the design shape shows the importance of the original parafoil design and the manufacturing process.

The scanned 3-D images as shown in Fig. 7 provide a data set to calculate the surface area and volume of each cell and the added air mass of the parafoil. Using the mathematical method developed for the parafoil, the calculated surface area and volume of each of the 14 cells from three separate scans and their averages are shown in Figs. 9 and 10. The median surface area and volume of the 14 cells were then calculated from the averages. Their values are tabulated in Table 3 and shown as dotted lines in Figs. 9 and 10. In addition to the individual cell surface and volume calculations, the total parafoil surface and volume were also calculated directly from the three scans. The results are also tabulated in Table 3 for comparison with those from individual cell calculation. It is seen that the total parafoil surface areas calculated from both methods are quite close. But the total parafoil volume calculated from individual cell volumes is about 3% higher than that calculated from the direct volume scan. This is expected because of the finite curvature of the parafoil. Additional volume is introduced when the volume of each cell is obtained by vertical projection as described earlier and when the individual cell volumes are added. The total cell volume of 4.641 cm^3 corresponds to an air mass of 1.04 kg (2.29 lb). Using an average canopy loading density (payload weight/parafoil top surface area) of 7.32 kg/m^2 (1.5 lb/ft^2), the payload weight of the parafoil becomes 8.4 kg (18.5 lb). The ratio between the added air mass and the payload mass becomes 12.3%. This ratio is much less than those for round parachutes.

When a turn of a parafoil is desired during flight, the trailing edge of the side toward the turn direction side is pulled down to increase

Table 2 Calibration data of the 3-D scanning apparatus

	Theoretical values	Mesh model	Contour model
Surface area, cm^2	1956	1963	1938
Volume, cm^3	1217	1202	1200

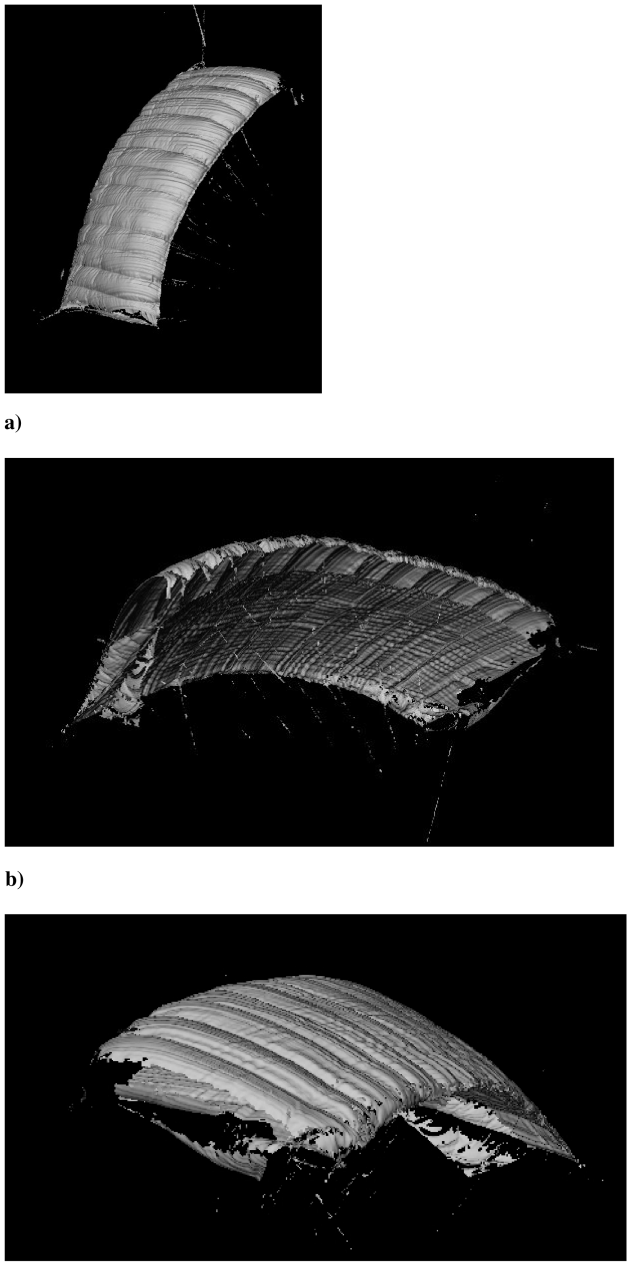

a)

b)

c)

Fig. 7 Typical scanned images of the parafoil.

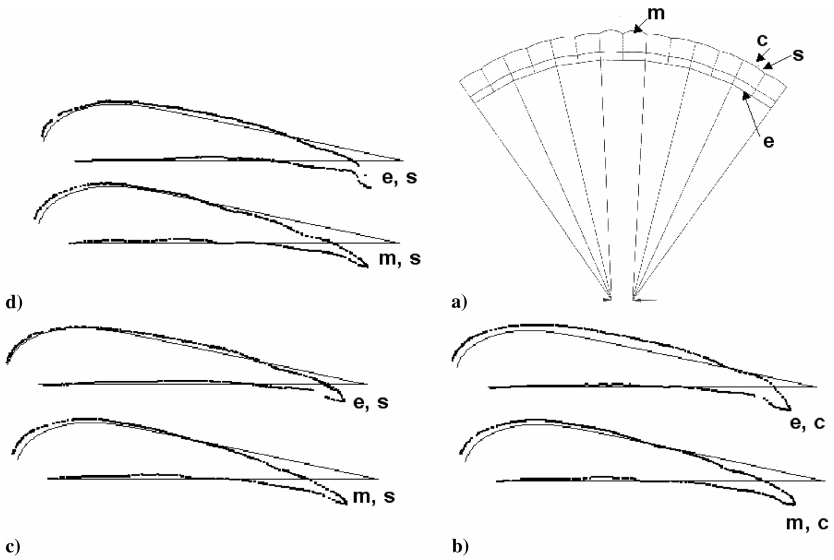

Fig. 8 a) Front design view of the 14-cell parafoil; b)–d) cross sections of scanned cells and cross sections of cell design: m—middle cell, e—end cell, c—center of cell, s—side of cell.

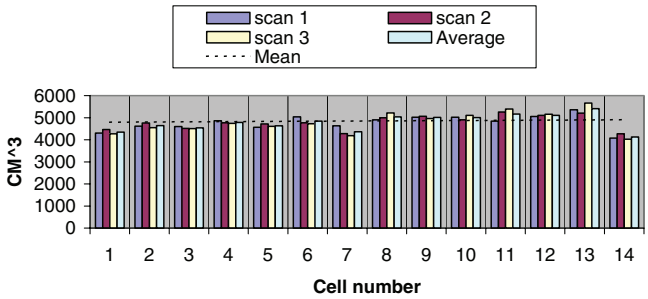

Fig. 9 Parafoil cell surface area of parafoil from 3-D scan.

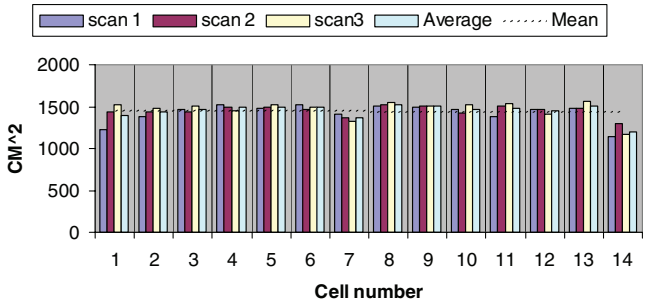

Fig. 10 Parafoil cell volume of parafoil from 3-D scan.

the drag force on that side in order to make the turn. The parafoil with a pull-down trailing edge and a cross section of the cell with the pull-down trailing edge are shown in Fig. 11. It is seen that while the trailing end of the cell is pulled down, the main body of the cell remains unchanged. During an actual flight, the pull down will increase the angle of attack of the cells being pulled down, which will increase the lift. Therefore, the resultant drag force is accompanied by an increase in the lift force during a trailing edge pull down. Similarly, a lift force is also generated during a canopy flare for landing when the entire trailing edge is pulled down. For an efficient turn or landing, the additional lift force is undesirable and additional means to suppress this lift force will enhance the turn or landing performance. The observed pull-down cross section tends to support the need to decrease the undesirable lift during a turn or landing.

Round Parachutes (RP)

Three images of RP1 from the scan are shown in Fig. 12. As shown in the parafoil scan, voids in the surface scan are shown in black. From these 3-D images, cross sections through the canopy apex were obtained. A typical cross section is shown in Fig. 13a. At the skirt, the least-square method was used to determine the diameter of the circle from the actual scan of the canopy (Fig. 13a). For comparison, a circle with this diameter is shown with the cross section of the canopy (Fig. 13b). The deviation of the canopy cross section from that of a circle is clearly seen. It is found that the cross section obtained from a combination of a thin circular disk and an oblate spheroid matches very well with the scanned canopy cross section, as shown in Fig. 13b. The dimensions of the disk and the oblate spheroid are shown in Table 4. This finding was also found for the cross sections of a full-scale 8.54-m diam personnel parachute and a 30.5-m diam cargo parachute [9]. This shows the usefulness of studying small-scale models for full-scale parachute geometric investigation.

As mentioned earlier, mathematical and computational techniques were developed and used to calculate the surface area and volume of the round parachutes from the scans shown in Fig. 12. Results for RP1 are shown in Table 4 along with those obtained from the oblate spheroid/circular disk geometry for comparison.

Because it is a flat circular parachute, the finished fabric surface area of the 1.7-m diam canopy was directly calculated to be 1.07 m^2. Because the parachute was inflated at a low velocity of 6.7 m/s, there were wrinkles in the canopy fabric. This is most likely the major reason for the lower surface area values obtained from the direct scan and the semi-oblate spheroid/circular disk (Table 4). In addition, the geometric approximation for the void areas in the scan also contributes to the errors. However, in spite of these difficulties, the

Table 3 Surface area and volume of model parafoil

	Surface area, m^2		Volume, m^3	
	Median of 14 cells	Total of 14 cells	Median of 14 cells	Total of 14 cells
From individual cell calculation	0.145	0.0203	0.479	0.067
From direct parafoil calculation	0.146	0.0204	0.464	0.065

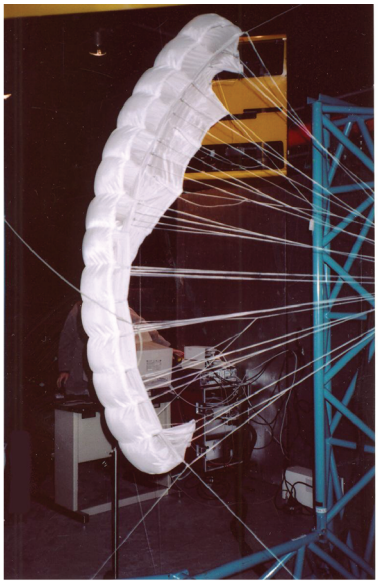

a)

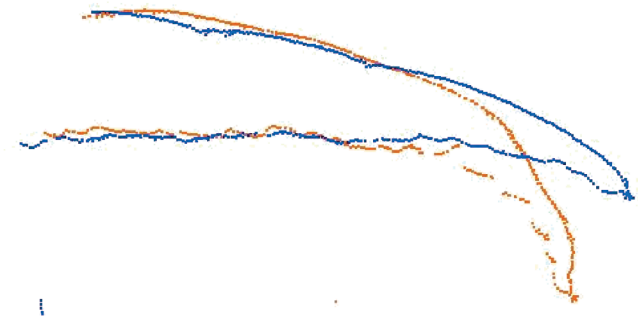

b)

Fig. 11 a) Pull down of trailing edge on one side of parafoil; b) comparison of cross sections between a cell with pull-down trailing edge and a cell without.

semi-oblate spheroid/circular disk approximation gives a reasonably good estimate.

The effect of fabric porosity on the canopy geometry and parachute performance has always been an important but relatively unknown area. The two round parachutes, RP2 and RP3, made from porous and nonporous fabrics, respectively, were constructed and scanned to investigate their geometry. Cross sections of the two canopies from the scan are shown in Fig. 14. It is seen that there are virtually no differences. The strain of the canopy was estimated by assuming the canopy to be a thin-walled homogeneous hemispherical vessel and the air pressure to be the stagnation pressure at 6.7 m/s for the nonporous canopy. The estimated strain was calculated to be very low at 0.2%.[‡] Because the air pressure for the porous canopy would be lower (due to airflow through the canopy fabric), its strain would be even lower than 0.2%. Such low strain values are beyond the measurement capability of the present 3-D laser scanning apparatus. Consequently, the two cross sections show virtually no differences.

When the vent of a round canopy is pulled down toward the skirt, the skirt area or the canopy projected area and the drag coefficient increase. This vent pull-down procedure is a standard method for increasing the drag force of Army cargo parachutes. Various amounts of vent pull down were performed on the round parachute RP1 and the corresponding canopy shapes were scanned. Cross sections of the canopy obtained from the scan are shown in Fig. 15a. The diameter of the skirt as a function of the amount of vent pull down determined from Fig. 15a is shown in Fig. 15b. It is seen that

[‡]Godfrey, T., U.S. Army Natick Soldier Center, Natick, MA, private communication, Jan. 2005.

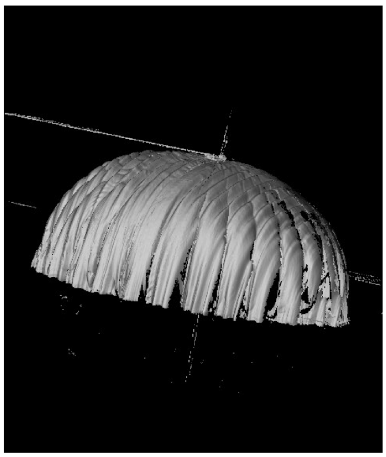

a)

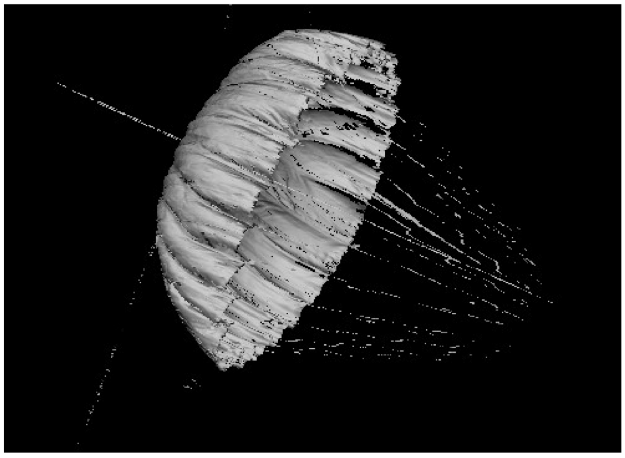

b)

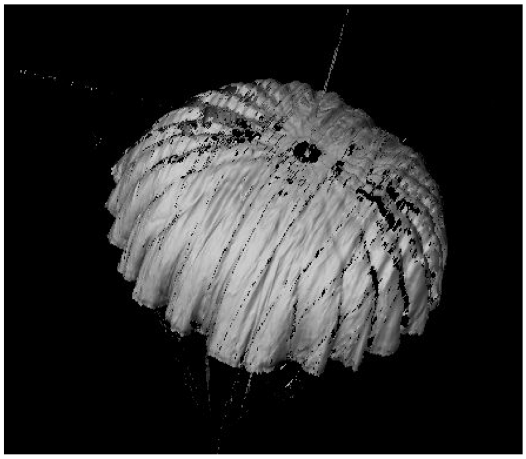

c)

Fig. 12 Typical scanned images of round parachute RP1.

Table 4 Surface area and volume measurements of round parachute RP1

	Surface area, m^2	Volume, m^3
Semi-oblate spheroid plus circular disk	0.923 Equatorial radius, $a = 0.425$ m Polar radius, $c = 0.263$ m Disk thickness = 0.052	0.130
From direct scan	0.861	0.126
From constructed diameter	1.07	——

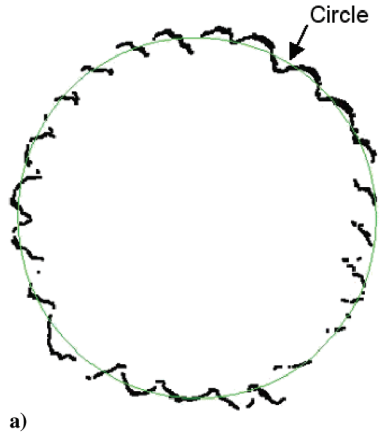

a)

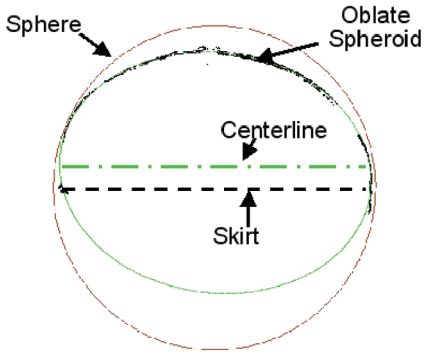

b)

Fig. 13 a) Skirt contour of round parachute RP1 from 3-D scan, and its circumference from least-square fit; b) canopy cross section of round parachute RP1 and its comparison with cross sections of an oblate spheroid and sphere.

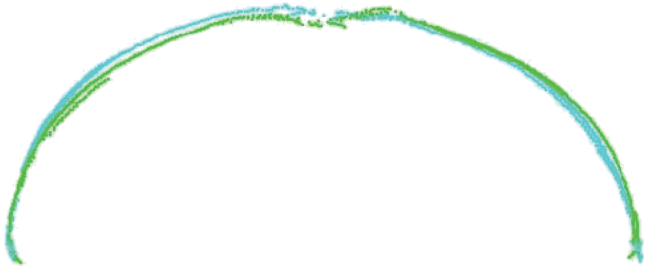

Fig. 14 Comparison of cross sections between round parachute RP2 (green) and RP3 (blue).

the skirt diameter increases as the amount of vent pull down increases. The maximum diameter increase occurs at about 305 mm of vent pull down when the vent is almost at the skirt. Beyond that, the diameter begins to decrease. The amount of 305-mm vent pull down corresponds to 26% of the constructed canopy diameter (1170 mm). A side view of the canopy at 26% vent pull down from the scan is shown in Fig. 16a. For comparison with full-scale parachutes, a fully inflated 21-m diam G12 Army cargo parachute with standard vent pull down is shown in Fig. 16b. For the G12 parachute, the standard amount of vent pull down also places the vent close to the skirt area. This amount of vent pull down corresponds to 24% of the constructed canopy diameter. The similarity between the two side views at the similar amount of vent pull down is striking. This shows the application of small-scale parachutes to predict the geometry of large-scale parachutes.

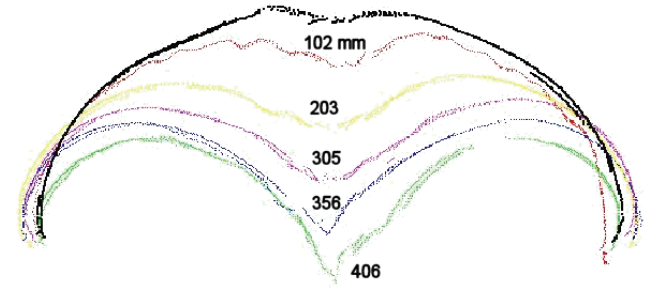

a)

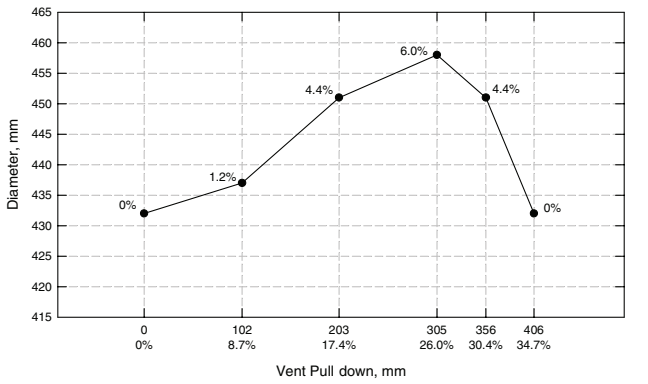

b)

Fig. 15 a) Canopy cross sections of round parachute RP1 with various amounts of vent pull down; b) change in projected diameter as a function of amount of vent pull down (% amount of pull down measured relative to the constructed canopy diameter; % change in diameter measured relative to the fully inflated projected diameter).

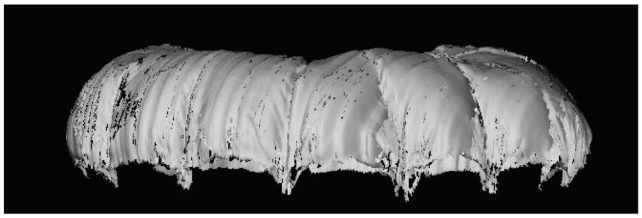

a)

b)

Fig. 16 Comparison of canopy profiles between a) model round RP1 and b) full-scale G12 cargo parachute, with vent pull down.

Ring-Slot Parachute

A scan and a cross section of the ring-slot parachute are shown in Fig. 17. Comparison of the cross section with that of the round parachute RP2 shows that the two cross sections are similar and the slots (geometric opening) apparently resulted in a slightly larger canopy than the round canopy.

Cross Parachutes

Because edges are much more difficult to scan than continuous surfaces, it was difficult to scan the cross parachutes because of the numerous fabric edges on the canopy. In addition, at 6.7 m/s, the

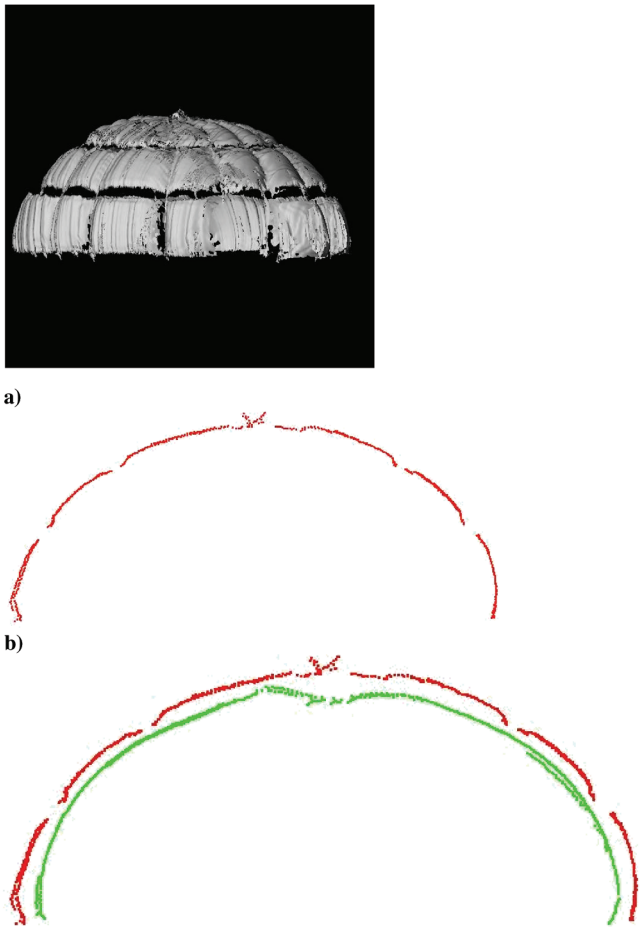

Fig. 17 a) Scanned image of ring-slot parachute; b) cross section of ring-slot parachute; c) comparison of canopy cross sections between ring-slot parachute and round parachute RP1.

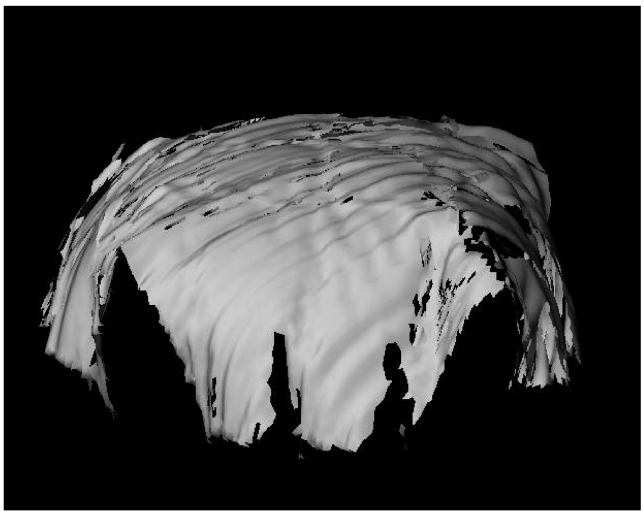

Fig. 18 Scanned image of cross parachute CP1.

canopy fabric had excessive wrinkles that resulted in many void areas (Fig. 18). Therefore, surface area and canopy volume could not be accurately determined from the scan. However, cross sections of the canopies were obtained from the scan and are shown in Fig. 19. It is seen that all three cross parachutes show similar cross sections. The cross section of the round parachute RP2 (Fig. 13a) was geometrically scaled and superimposed on the cross section of the cross parachute with a vent. It is seen in Fig. 20 that the top portion of

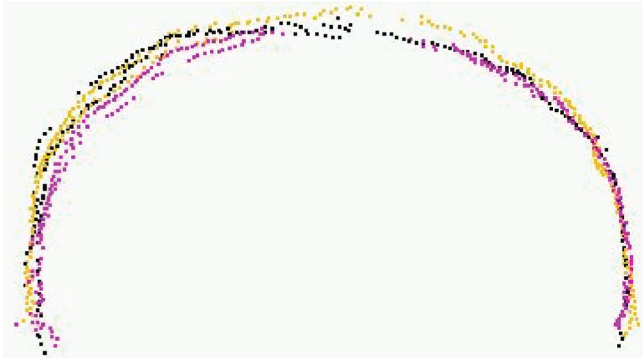

Fig. 19 Comparison of canopy cross sections among three cross parachutes.

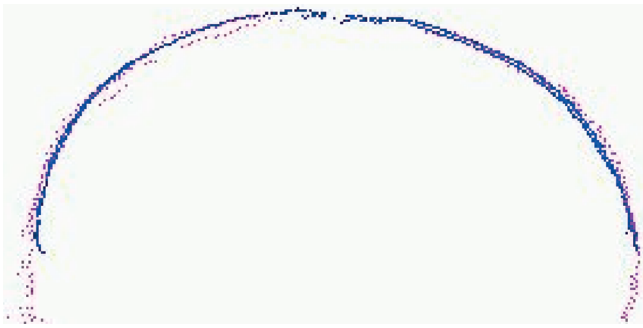

Fig. 20 Comparison of canopy cross sections between cross parachute CP1 and round parachute RP1.

the cross parachute canopy shows a similar profile as that of the round parachute. The similarity seems to be reasonable because the top portion of the canopy of cross parachutes is basically like the canopy of round parachutes.

Conclusions

We have demonstrated the feasibility and application of using a 3-D laser scanning technique to investigate the geometry of model parachutes. Along with the experimental technique, mathematical methods have been developed to analyze the scan data to determine the geometry, surface area, and volume of parafoils and round parachutes. In addition, the scanned images also provide useful canopy cross sections that are difficult to obtain from other experimental techniques, such as photography or video analyses. The obtained cross sections provide valuable information for full-scale parachute performance and operation evaluation. Scanning of fully inflated parachutes at higher air velocities is recommended for future work in this area.

References

[1] Machin, R. A., Iacomini, C. S., Cerimele, C. J., and Stein, J. M., "Flight Testing the Parachute System for the Space Station Crew Return Vehicle," *Journal of Aircraft*, Vol. 38, No. 5, Sept.–Oct. 2001, pp. 786–799.

[2] Cockrell, D. J., "The Aerodynamics of Parachutes," North Atlantic Treaty Organization, Advisory Group for Aerospace Research and Development, AGARDograph No. 295, Specialized Printing Services, Ltd., Loughton, Essex, England, 1987, pp. 34–41.

[3] Knacke, T. W., "Parachute Recovery Systems Design Manual," Para Publishing, P.O. Box 4232, Santa Barbara, CA 93140, 1992.

[4] Charles, R., Accorsi, M., Morton, S., Tomaro, R., Stein, K., Sathe, S., and Tezduyar, T., "Overview of the Airdrop Systems Modeling Project Within the Collaborative Simulation and Test (CST) Common High Performance Computing Software Support Initiative (CHSSI) Portfolio," AIAA Paper 2005-1621, May 2005.

[5] Tutt, B., and Taylor, T., "The Use of LS-DYNA to Simulate the Inflation of a Parachute Canopy," AIAA Paper 2005-1608, May 2005.

[6] Stein, K., Benney, R., Tezduyar, T., Leonard, J., and Accorsi, M., "Fluid-Structure Interaction of a Round Parachute: Modeling and

Simulation Techniques," *Journal of Aircraft*, Vol. 38, No. 5, Sept.–Oct. 2001, pp. 800–807.

[7] Oberkampf, W., and Roy, C., "Verification and Validation in Computational Simulation," AIAA Professional Development Short Course, 7–8 Jan. 2006, 1801 Alexander Bell Drive, Suite 500, Reston, VA 20191-4344.

[8] Heinrich, H. G., and Noreen, R. A., "Analysis of Parachute Opening Dynamics with Supporting Wind-Tunnel Experiments," *Journal of Aircraft*, Vol. 7, No. 4, July–Aug. 1970, pp. 341–347.

[9] Berndt, R. J., "Experimental Determination of Parameters for the Calculation of Parachute Filling Times," Flight Dynamics Laboratory, Wright–Patterson Air Force Base, Ohio, USA, Jahrbuch 1964 WRLR, pp. 299–316.

[10] Matos, C., Mahalingham, R., Ottinger, G., Klapper, J., Funk, R., and Komerath, N., "Wind Tunnel Measurements of Parafoil Geometry and Aerodynamics," AIAA Paper 98-0606, Jan. 1998.

[11] Ellson, R. N., and Nurre, J. H., Chairs/Editors, "Three-Dimensional Image Capture," *Proceedings of the International Society for Optical Engineering*, SPIE, San Jose, CA, 1997, Vol. 3023.

[12] Paquette, S., Corner, B. D., Brantley, J. D., and Li, P., "Anthropometric Data Extraction from 3-D Whole Body Scans," *International Ergonomics Association/Human Factors and Ergonomics Association Society 2000 Conference*, HFES, San Diego, CA, July 2000.

[13] Lee, C. K., Kim, I. Y., and Wood, Alycia, "Investigation and Correlation of Manikin and Bench-Scale Testing of Clothing Systems," *Fire and Materials*, Vol. 26, 2002, pp. 269–278.

[14] Johari, H., and Desabrais, K., "Stiffness Scaling for Solid-Cloth Parachutes," *Journal of Aircraft*, Vol. 40, No. 4, July–Aug. 2003, pp. 631–638.

[15] Lee, C. K., "Modeling of Parachute Opening: An Experimental Investigation," *Journal of Aircraft*, Vol. 26, No. 5, May 1999, pp. 444–451.

[16] Li, P., Lee, C., and Corner, B., "Computing Surface Area and Volume of Parachutes from 3D Scans," *Engineering Computation: International Journal for Computer-Aided Engineering and Software*, Vol. 22, Nos. 3–4, 2005, pp. 393–408.

[17] Hoppe, H., DeRose, T., Duchanp, T., McDonald, J., and Stuetzle, W., "Surface Reconstruction from Unorganized Points," *Proceedings of SIGGRAPH 1992*, ACM Press, Boston, MA, 1992, pp. 71–78.

[18] Liao, C. W., and Medioni, G., "Surface Approximation of a Cloud of 3D Points," *Graphical Modes and Image Proceedings*, Vol. 57, No. 1, Jan. 1995, pp. 67–74.

[19] Curless, B., and Levoy, M., "A Volumetric Method for Building Complex Models from Range Image," *Proceedings of SIGGRAPH 1996*, ACM Press, Boston, MA, 1996, pp. 303–312.

[20] Meyers, D., Skinner, S., and Sloan, K., "Surface from Contours," *Association for Computing Machinary Transactions on Graphics*, Vol. 11, No. 3, July 1992, pp. 228–258.